Inorganic Chemistry

Article

pubs.acs.org/IC

Structural Impact of Platinum on the Incommensurably Modulated γ-Brass Related Composite Structure $Pd_{15}Zn_{54}$

Partha P. Jana* and Sven Lidin

CAS Chemical Centre, Lund University, Getingevägen 60, Lund, Sweden, Box 124, SE-22100

Supporting Information

ABSTRACT: The crystal structure of three incommensurately modulated γ-brass related composite structures in the Pd−Zn−Pt system has been solved from X-ray single crystal diffraction data using a 3 + 1-dimensional super space description. The compounds $Pt_xPd_{15-x}Zn_{54}$ ($x \approx 6, 7, 10$) crystallize in orthorhombic superspace group $Fmmm(\alpha 00)0s0$ (F = [(1/2, 1/2, 0, 0); (1/2, 0, 1/2, 0); (0, 1/2, 1/2, 0)] with the following fundamental cell dimensions: a = 4.265(1) Å, b = 9.132(1) Å, c = 12.928(2) Å, $q \approx 0.629a^*$; a = 4.284(1) Å, b = 9.151(2) Å, c = 12.948(4) Å, $q \approx 0.628a^*$; and a = 4.288(1) Å, b = 9.140(4) Å, c = 12.926(7) Å, $q \approx 0.627a^*$. Each structure is built by two sub-lattices—pentagonal antiprismatic columns parallel to [100] and a zigzag chain of Zn atoms running along the center of the column.

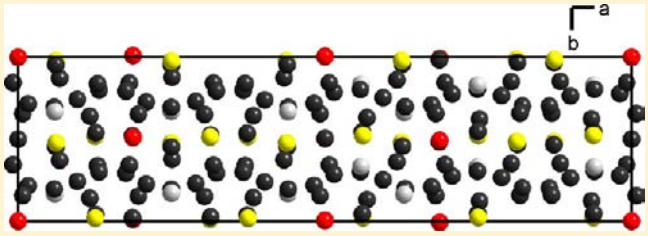

INTRODUCTION

The γ-brass phases are of particular interest to our investigation for their structural complexity and their stabilization mechanism. γ-brass phases are part of a special class of intermetallic compounds, in which the formation of a particular structure occurs at a certain value of ratio of valence electrons to atom (e/a, vec), i.e., 21:13, which was first recognized by Hume−Rothery in 1926.[1−3] In fact, the condition is valid irrespective of the nature of the constituent metals. There are various compounds such as Cu_5Zn_8[4] and Cu_9Al_4[5,6] which adopta γ-brass structure at vec values equal to 21:13 per atom. It has recently been shown by calculations that these structures are indeed electronically stabilized at this vec value.[7−9]

Compounds having general composition M_2Zn_{11} (M = Ni,[10] Pd,[11] Pt,[12]) and an e/a ratio of 21:13 (assigning the valency zero to transition metals and two to zinc) all form γ-brass type structures. The existence and the compositions of γ-brass type structures have been confirmed in systems such as Fe−Zn (Fe_3Zn_{10}),[13] Ni−Zn (Ni_2Zn_{11}),[10] Cu−Zn ($Cu_{5-x}Zn_{8+x}$),[4,14,15] Pd−Zn ($Pd_{2+\delta}Zn_{11-\delta}$),[11,16] Rh−Zn ($Rh_2Zn_{11}$),[17] Ir−Zn ($Ir_2Zn_{11}$),[18] and Pt−Zn ($Pt_2Zn_{11-\delta}$).[11,12] However, the binary phase spaces in close vicinity[16,19−21] to the γ-brass region accommodate bundles of phases with bewildering compositional and structural complexity.

Perhaps most complex among the γ-brass related structures are the incommensurate composites which have recently been revealed in some Cd-[22] and Zn-rich phases.[23]

Morton revealed by electron microscopy studies that the γ-brass regions of Ni−Zn,[24] Cu−Zn,[25] and Pd−Zn[26] do not only accommodate the γ-brass phase but also structurally related, complex phase bundles with lower symmetry. A series of six γ-brass and γ-brass-related structures in the Pd−Zn system was identified by Gourdon and Miller using single crystal structure determination.[16]

Among them, the cubic $Pd_{2.35}Zn_{10.65}$ (<20% Pd)[16] phase adopts a Hume−Rothery γ-brass structure with a lattice parameter $a \approx 9.1$ Å in the body centered cubic space group $I\bar{4}3m$. Those phases that exceeded 20% Pd (five out of six phases) could approximately be indexed with either an F- or C-centered orthorhombic Bravis lattice. An example of those closely related orthorhombic phases is $Pd_{15}Zn_{54}$. A single crystal structure of the $Pd_{15}Zn_{54}$ phase has been reported by Armbrüster et al.[27] and refined in the space group *Cmce* with lattice parameters a = 12.9095(5) Å, b = 9.1096(4) Å, and c = 34.047(1) Å. The phase was re-examined by Gourdon and Miller,[16] who proposed that the composition of the phase $Pd_{25}Zn_{75}$ is more precisely $Pd_{24.2}Zn_{75.8}$. According to them, the structure crystallizes in the centric orthorhombic space group *Cmce* with cell parameters a = 12.929(3) Å, b = 9.112(4) Å, and c = 33.32(1) Å. Moreover, the structure can also be refined with the 3 + 1D formalism with the orthorhombic superspace group $Xmmm(00\gamma)0s0$ with the lattice parameters a = 12.929(3), b = 9.112(4), c = 2.5631(7), $q \approx (8/13)c^*$.

On account of this background, we investigate the platinum substituted $Pd_{15}Zn_{54}$ to understand how substitution by Pt atoms can influence the structural stability and chemical compositions of γ-brass phases related to $Pd_{15}Zn_{54}$. No phase has been reported in the Pt−Pd−Zn ternary system to date.

In this study, attempts were made to synthesize various $(Pt_xPd_{15-x})Zn_{54}$ targets with nominal composition ranging from 0 to 15 atom % of platinum. The structures were solved from single crystal X-ray diffraction intensities. We present here

Received: June 24, 2012
Published: September 5, 2012

   dx.doi.org/10.1021/ic301326p | *Inorg. Chem.* 2012, 51, 9893−9901

Table 1. Crystallographic and Technical Data for the Single Crystal Structure Refinements of $Pt_xPd_{15-x}Zn_{54}$ with $x \approx 6$, 7, and 10

formula (synthesis)	$Pt_xPd_{15-x}Zn_{54}$ (C1) with $x = 6$	$Pt_xPd_{15-x}Zn_{54}$ (C2) with $x = 7$	$Pt_xPd_{15-x}Zn_{54}$ (C3) with $x = 10$
formula (XRD)	$Pt_{1.14}Pd_{2.86}$ $Zn_{26.89}(Pt/Pd)_{3.63}$	$Pt_{1.50}Pd_{2.50}Zn_{26.55}(Pt/Pd)_{3.97}$	$Pt_{2.00}Pd_{2.00}Zn_{26.77}(Pt/Pd)_{3.74}$
formula (EDS)	$Pt_{6.0(4)}Pd_{9.3(3)}Zn_{54.7(6)}$	$Pt_{7.3(4)}Pd_{8.5(6)}Zn_{54.3(4)}$	$Pt_{9.9(5)}Pd_{5.0(2)}Zn_{54.8(3)}$
cryst syst		orthorhombic	
space group type		$Fmmm(\alpha 00)0s0$	
a (Å)	4.265(1)	4.284(1)	4.288(1)
b (Å)	9.132(1)	9.151(2)	9.140(4)
c (Å)	12.928(2)	12.948(4)	12.926(7)
V (Å^3)	503.54(11)	507.6(2)	506.6(4)
modulation wave vector	0.6286(5)	0.6276(2)	0.6273(4)
crystal color		silvery with metallic luster	
data collection			
diffractometer		XCalibur four-circle diffractometer	
radiation		Mo Kα	
monochromator		graphite	
T/K	293(2)	293(2)	293(2)
Θ range	3–28.92	2.99–29.18	2.99–29.04
reflns measured	19491	12319	26583
independent reflns	1156	1145	1161
obsd reflns ($I > 3\sigma(I)$)	848	984	991
index range	$-5 \le h \le 5$	$-5 \le h \le 5$	$-5 \le h \le 5$
	$-12 \le k \le 12$	$-12 \le k \le 12$	$-12 \le k \le 12$
	$-17 \le l \le 17$	$-17 \le l \le 17$	$-17 \le l \le 17$
data reduction/absorption correction		multiscan	
R_{int}	0.058	0.0468	0.0664
structure solution, refinement		*JANA* 2006 program package[28]	
structure solution		Superflip[29]	
structure refinement on		(F^2)	
$R[F^2 > 2\sigma(F^2)]$, wR (F^2), S	0.0319, 0.1043, 1.36	0.0335, 0.0900, 2.09	0.0440, 0.1011, 2.27
R_{main}	0.0182	0.0230	0.0301
$R_{satellite,}$			
first order	0.0327	0.0334	0.0462
second order	0.0576	0.0486	0.0615
third order	0.0894	0.0807	0.1004
no. of reflns	1156	1145	1161
no. of params	79	79	79
k^a	0.0016	0.0004	0.0004
$\Delta\rho_{min}/\rho_{max}$ (eÅ^{-3})	−3.03/3.14	−3.82/4.01	−4.27/4.27

[a]Weighting scheme based on measured s.u.'s w = $1/[\sigma^2(I) + kI^2)$

the structure of three incommensurately modulated compounds $Pt_xPd_{15-x}Zn_{54}$ ($x \approx 6$, 7, 10) from single crystal X-ray diffraction data using a 3 + 1D super space description.

RESULTS AND DISCUSSION

Structural Solution. The diffraction patterns display strong main reflections and additional satellite reflections. Diffraction data are metrically orthorhombic and follow an F-centered lattice. Data sets were averaged according to the *mmm* point group. The diffraction patterns indicate a basic cell with cell dimensions $a = 4.265(1)$ Å, $b = 9.132(1)$ Å, $c = 12.928(2)$ Å. Many additional satellite reflections indicate a superstructure along the [100] direction. The satellite reflections could be indexed by one q vector along the a^* direction, $q = \alpha a^*$. The value of α is approximately equal to 0.629 for $(Pt_xPd_{15-x})Zn_{54}$ (where $x \approx 6$). Additional systematic absence for satellites indicates a super space translation of 1/2 associated with the m mirror plane perpendicular to [010], and the (3 + 1)D superspace group was considered to be $Fmmm(\alpha 00)0s0$. Satellites of up to third order were detected with the criteria for observed reflection (3σ). The structure was solved and refined by the Jana 2006 program package.[28,29] The possible positions of missing zinc atoms were taken from difference Fourier synthesis maps. The structure solution and subsequent refinement yielded four atomic positions in the asymmetric unit. Modulations on all four positions were checked using Fourier maps. M1 (1/2, 0, 0), M′1 at (1/2, ∼1/7, ∼1/6), and Zn2 (0, 0, ∼1/8) are well modeled, but the position Zn3 is problematic. On the basis of this, we tried to find a composite model of Zn3. The first subsystem (*vide infra*, W^1) consists of three atoms, M1 at (1/2, 0, 0), M′1 at (1/2, ∼1/7, ∼1/6), and Zn2 (0, 0, ∼1/8), and the second subsystem (*vide infra* W^2) consists of one Zn3 atom at (3/4, 1/4, 0). The two subsystem reflection sets are obtained from the (3 + 1)D superspace reflection indices defined by the matrices:

$$W^1 = \begin{pmatrix} 1 & 0 & 0 & 0 \\ 0 & 1 & 0 & 0 \\ 0 & 0 & 1 & 0 \\ 0 & 0 & 0 & 1 \end{pmatrix} \text{ and } W^2 = \begin{pmatrix} 1 & 0 & 0 & 0 \\ 0 & 1 & 0 & 0 \\ 0 & 0 & 1 & 0 \\ 1 & 0 & 0 & 1 \end{pmatrix}$$

dx.doi.org/10.1021/ic301326p | *Inorg. Chem.* 2012, 51, 9893–9901

Note that this setting is equivalent to that used by Gourdon et al.[23] Each sublattice contains specific subsets of main and satellite reflections, and there are some reflections which are satellites in both sublattices. Anisotropic displacement parameters of the atoms and extinction correction were taken into account at this stage. The possibility of Pd and Pt at (1/2, 0, 0) occupancy modulations was observed by analyzing Debye–Waller factors. One position gave indications of such behavior, and for this position Pd and Pt were set to fill the site completely via complementary occupation modulation. The two atoms were constrained to have the same displacive modulation and the same thermal parameters. Moreover, this was also useful to model the occupationally modulated atom at (1/2, ∼1/7, ∼1/6) where M′1 is an alteration between a mixed (Pt/Pd)1 (in a fixed ratio and hence modeled as a Nd1 atom) and a Zn1 atom to get a more physical model. The atoms (Pd1/Pt1, (Pd/Pt)1/Zn1, Zn2, and Zn3) were further modeled with positional displacement waves. Modulation waves of thermal displacement parameters were applied to all the atoms. Details concerning the data collection, atomic coordinates, equivalent isotropic displacement parameters, and anisotropic displacement parameters are listed in Tables 1–5. This refinement model using 3 + 1D superspace group allows us to refine the compounds $(Pt_xPd_{15-x})Zn_{54}$ (where $x \approx 7$, 10) using similar basic cells $a = 4.284(1)$ Å, $b = 9.151(2)$ Å, $c = 12.948(4)$ Å and $a = 4.288(1)$ Å, $b = 9.140(4)$ Å, $c = 12.926(7)$ Å, in $Fmmm(\alpha 00)0s0$ with $q = 0.628a^*$ and $q = 0.627a^*$, respectively. Note that for the compounds $(Pt_xPd_{15-x})Zn_{54}$ (where $x \approx 7$, 10), the M′1 atom at (1/2, ∼1/7, ∼1/6) is occupationally modulated between a mixed (Pt/Pd)1 and a Zn1 atom. To get a physical model, the fixed ratios of (Pt/Pd)1 are modeled as a Pm1 and a Ho1, respectively.

The ternary phase $Pt_xPd_{15-x}Zn_{54}$ ($x \approx 6$, 7, and 10) was studied by means of preparative methods, X-ray diffraction. Single crystal X-ray structure and EDS analyses are essentially in accord with the nominal compositions.

Structural Discussion. From the diffraction pattern only, the classification of a crystal structure as either commensurately or incommensurately modulated is not an entirely trivial distinction. It is difficult to determine whether or not the modulation vector is truly commensurate or incommensurate with

Table 2. Structural Data for $Pt_xPd_{15-x}Zn_{54}$ with $x \approx 6$, 7, and 10

atom	x	y	z	occ.	U_{eq}[a]/Å^2
Pd1	0.5[b]	0	0	0.715(7)	0.0096(2)
				0.624(6)	0.0091(2)
				0.498(7)	0.0096(2)
Pt1	0.5	0	0	0.285(7)	0.0096(2)
				0.376(6)	0.0091(2)
				0.502(7)	0.0096(2)
(Pt/Pd)1	0.5	0.15120(6)	0.17947(5)	0.227(4)	0.0136(2)
		0.15108(6)	0.17957(4)	0.248(4)	0.0133(2)
		0.15099(7)	0.17961(5)	0.233(4)	0.0138(3)
Zn1	0.5	0.15120(6)	0.17947(5)	0.773(4)	0.0136(2)
		0.15108(6)	0.17957(4)	0.752(4)	0.0133(2)
		0.15099(7)	0.17961(5)	0.767(4)	0.0138(3)
Zn2	0	0	0.12349(8)	1	0.0158(3)
			0.12342(7)		0.0156(3)
			0.12341(9)		0.0165(4)
Zn3	0.75	0.25	0	1	0.0156(3)
					0.0149(3)
					0.0155(4)

[a] U_{eq} is defined as one-third of the trace of orthogonalized U_{ij} tensor. [b] Structural data given in the top to bottom lines refer to crystals C1, C2, and C3, respectively.

Table 3. Anisotropic Thermal Displacement Parameters U_{ij} (Å^2) for $Pt_xPd_{15-x}Zn_{54}$ with $x \approx 6$, 7, and 10

atom	U_{11}	U_{22}	U_{33}	U_{12}	U_{13}	U_{23}
Pt1/Pd1	0.0106(4)	0.0099(4)	0.0082(4)	0	0	0
	0.0103(4)	0.0081(4)	0.0088(4)	0	0	0
	0.0090(4)	0.0116(4)	0.0082(4)	0	0	0
(Pt/Pd)1/Zn1	0.0156(4)	0.0138(4)	0.0114(4)	0	0	−0.0033(2)
	0.0150(4)	0.0126(4)	0.0124(4)	0	0	−0.00358(19)
	0.0134(5)	0.0160(5)	0.0119(4)			−0.0030(2)
Zn2	0.0106(5)	0.0185(6)	0.0183(6)	0	0	0
	0.0105(5)	0.0176(5)	0.0186(5)	0	0	0
	0.0090(6)	0.0216(7)	0.0189(6)	0	0	0
Zn3	0.0185(6)	0.0135(5)	0.0147(6)	0	0	0
	0.0183(6)	0.0114(5)	0.0149(6)	0	0	0
	0.0169(7)	0.0153(6)	0.0142(6)	0	0	0

Table 4. Fourier Amplitude of the Occupancy Modulation[a] Function for $Pt_xPd_{15-x}Zn_{54}$ with $x \approx 6$, 7, and 10

	$n = 1$		$n = 2$		$n = 3$	
atom	$c1$	$s1$	$c2$	$s2$	$c3$	$s3$
Pd1/Pt1	0	0	∓0.293(5)	0	0	0
			∓0.335(5)			
			∓0.395(6)			
(Pt/Pd)1/Zn1	0	∓0.381(4)	∓0.246(3)	0	0	±0.103(3)
		∓0.420(4)	∓0.276(3)			±0.121(2)
			∓0.263(3)			±0.124(2)
		∓0.407(4)				

[a] Occupancy modulation function is defined by $P(\bar{x}_4^v) = P_0^v + \sum_{n=1}^{k} s_n \sin(2\pi n\bar{x}_4^v) + \sum_{n=1}^{k} c_n \cos(2\pi n\bar{x}_4^v)$.

dx.doi.org/10.1021/ic301326p | Inorg. Chem. 2012, 51, 9893–9901

Table 5. Fourier Amplitude of the Displacive Modulation Function for $Pt_xPd_{15-x}Zn_{54}$ with $x \approx 6$, 7, and 10

	C1			C2			C3		
	x	*y*	*z*	*x*	*y*	*z*	*x*	*y*	*z*
Pd1/Pt1								0.02497(11)	
s1		0.02422(11)			0.02462(10)				
s2	0.0035(2)			0.00319(17)			0.0039(2)		
s3		0.00149(10)			0.00128(8)			0.00077(10)	
M1/Zn1									
c1	−0.0666(2)			−0.0673(2)			−0.0677(3)		
s1		−0.01885(8)	0.00347(6)		−0.01914(8)	0.00348(5)		−0.01920(9)	0.00344(6)
c2		0.00519(8)	−0.00307(6)		0.00522(7)	−0.00311(5)		0.00548(9)	−0.00334(7)
s2	−0.0138(2)			−0.01341(16)			−0.0131(2)		
c3	0.0062(2)			0.00616(17)			0.0065(2)		
s3		0.00525(8)	−0.00151(7)		0.00480(7)	−0.00145(5)		0.00483(9)	−0.00150(6)
Zn2									
s1		0.05131(15)			0.05153(13)			0.05187(17)	
c2			0.00851(10)			0.00838(9)			0.00867(11)
s2	0.0131(3)			0.0128(3)			0.0129(4)		
s3		0.00400(18)			0.00324(15)			0.0032(2)	
Zn3									
s1		0.05665(15)			0.05653(14)			0.05670(18)	
s2	−0.0388(6)			−0.0378(5)			−0.0385(7)		
s3		0.00178(15)			0.00185(13)			0.00184(18)	

dx.doi.org/10.1021/ic301326p | Inorg. Chem. 2012, 51, 9893−9901

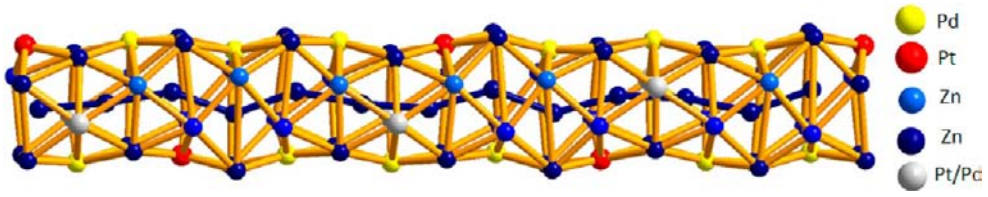

Figure 1. Commensurate approximation of the structure—$(Pd_xPt_{15-x})Zn_{54}$ (where $x \approx 6$) viewed along the c direction—the pentagonal antiprismatic column with a zigzag chain of Zn atoms running inside column. Zn atoms are shown in blue, Pt in red, Pd in yellow, and mixing of Pt/Pd in gray.

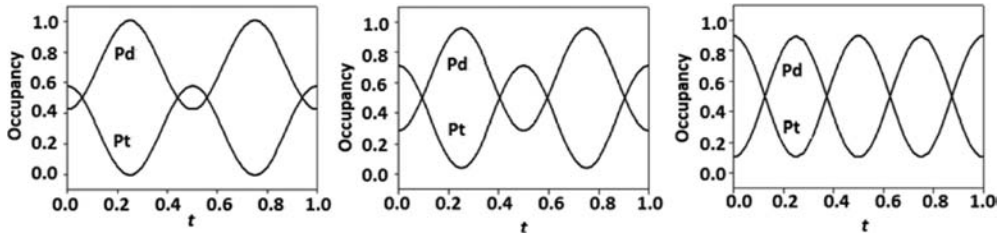

Figure 2. Occupancy modulations between Pd and Pt at (0 0 0) of $Pt_xPd_{15-x}Zn_{54}$ with $x \approx 6$, 7, and 10.

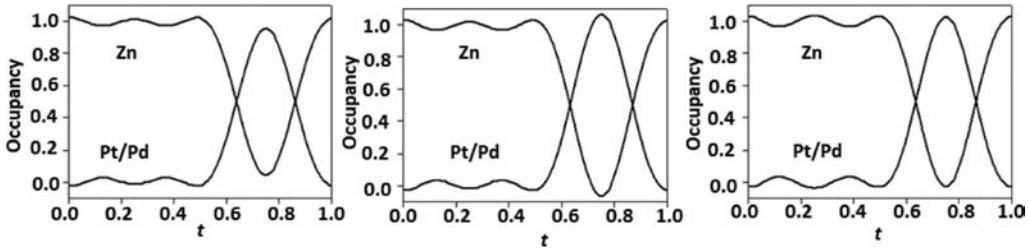

Figure 3. Occupancy modulations between Pt/Pd and Zn at (0, ~1/7, ~1/6) of $Pt_xPd_{15-x}Zn_{54}$ with $x \approx 6$, 7, and 10.

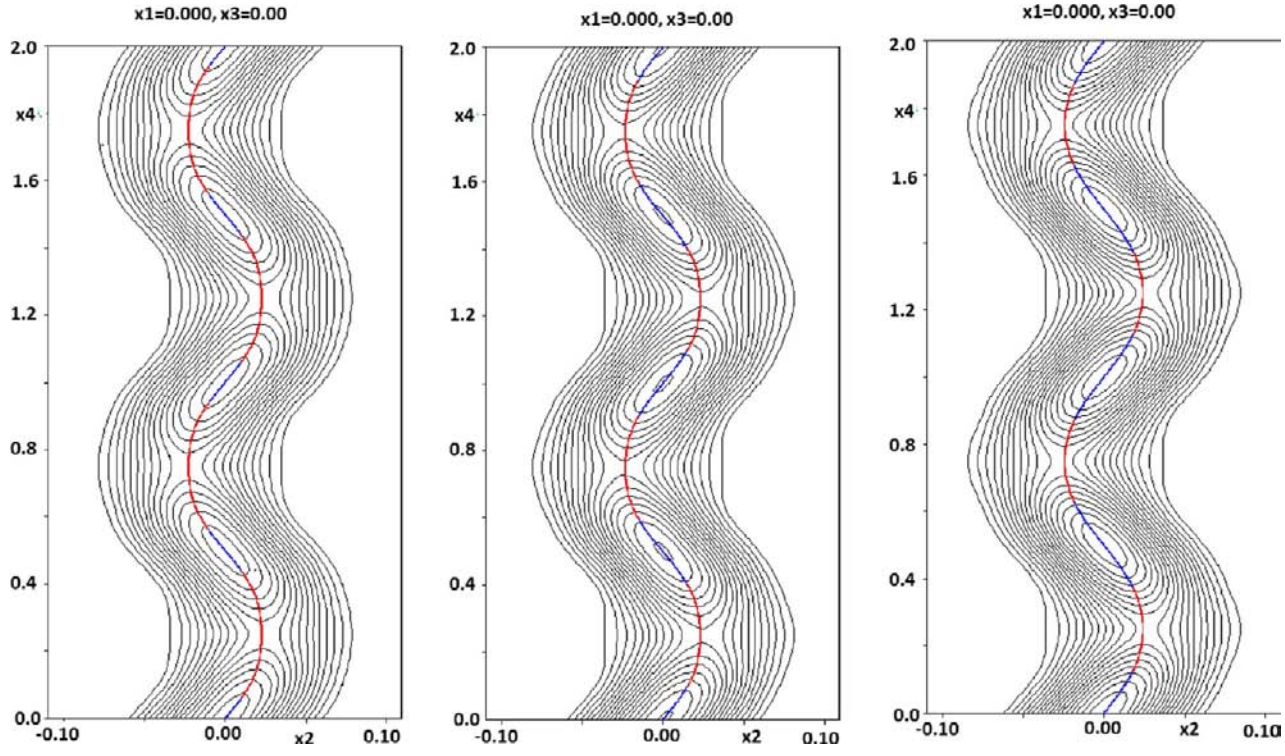

Figure 4. Electron density maps of Pd1 and Pt1 in the $Pt_xPd_{15-x}Zn_{54}$ (with $x \approx 6$ (left), 7 (middle), and 10 (right)) calculated from F(obs). The colored lines represent the refined modulation behavior of the Pd1 and Pt1 atoms.

dx.doi.org/10.1021/ic301326p | Inorg. Chem. 2012, 51, 9893−9901

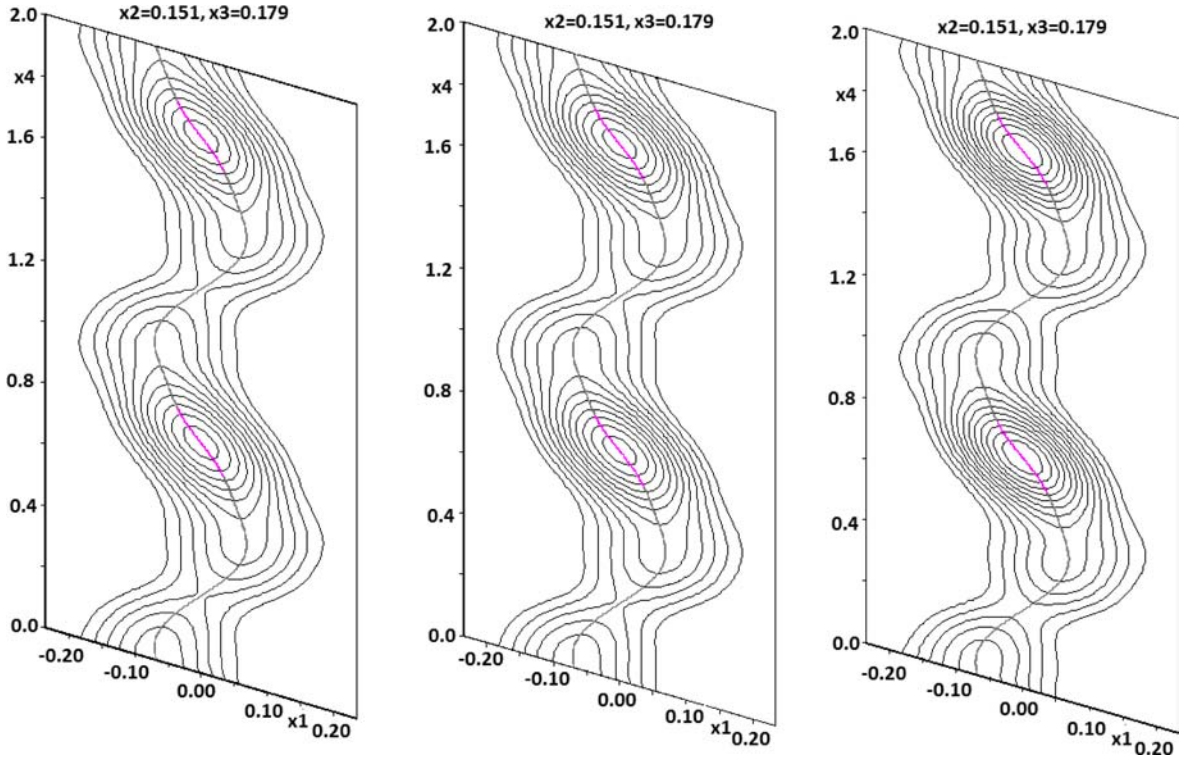

Figure 5. Electron density maps showing the modulation behavior of (Pt/Pd)1 and Zn1 in the $Pt_xPd_{15-x}Zn_{54}$ (with $x \approx 6$ (left), 7 (middle), and 10 (right)) calculated from F(obs). The colored lines represent the refined modulation behavior of the (Pt/Pd)1 and Zn1 atoms.

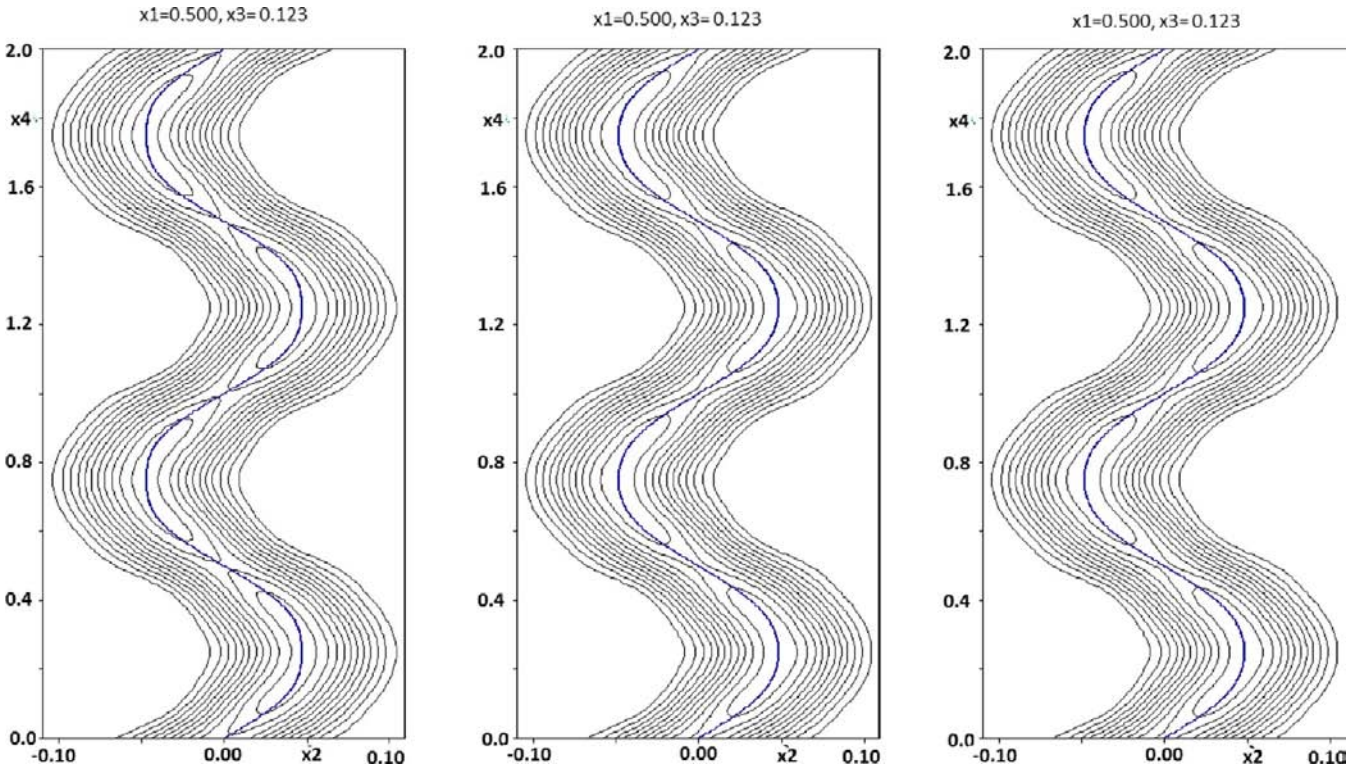

Figure 6. Electron density maps of Zn2 in the $Pt_xPd_{15-x}Zn_{54}$ (where $x \approx 6$ (left), 7 (middle), and 10 (right)) calculated from F(obs). The blue colored lines represent the refined modulation behavior of the Zn2 atom.

the basic vector because of the limitation of the resolution and the precision in the measuring process. In fact, it is always possible to describe an incommensurately modulated structure as a commensurate one. This requires an approximation of the wave vector by a commensurate one, i.e., approximating an irrational number by a well-chosen rational number. The procedure is not encouraged for a number of reasons. Low data to parameter ratios cause numerical instabilities and unstable

dx.doi.org/10.1021/ic301326p | Inorg. Chem. 2012, 51, 9893−9901

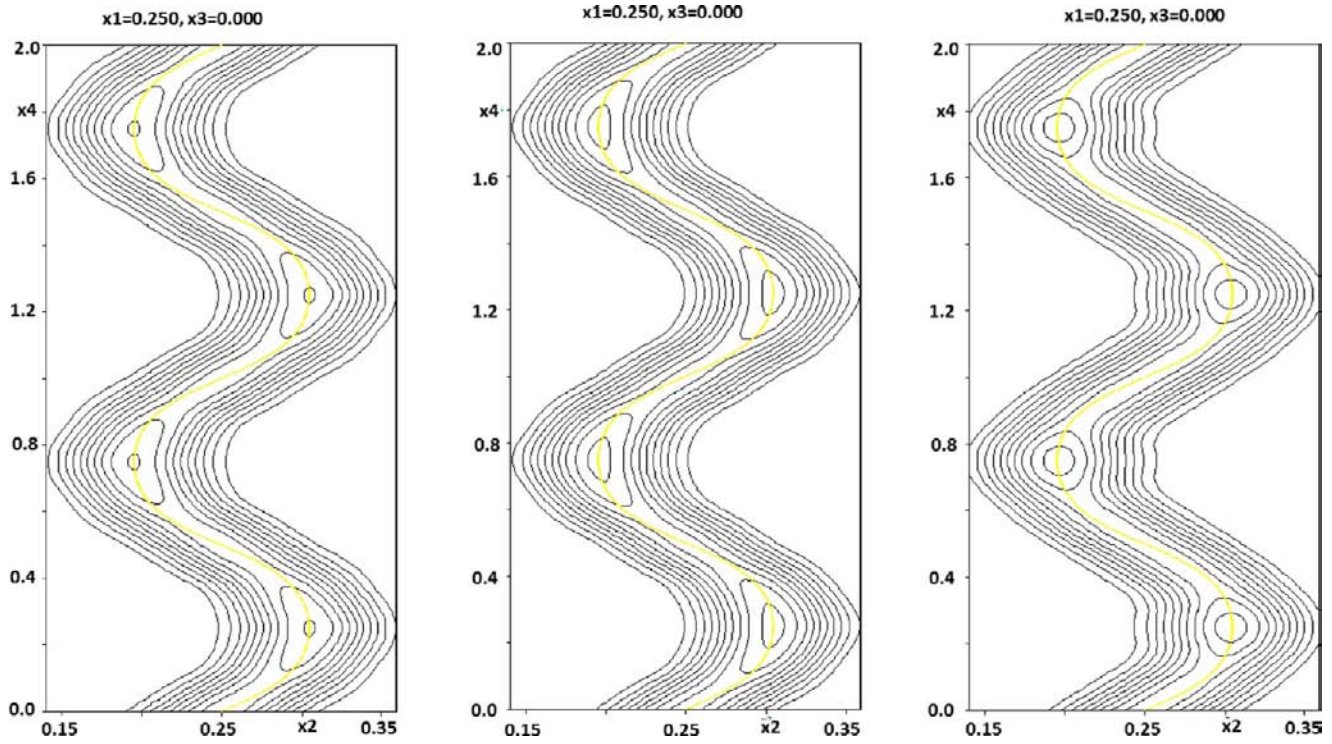

Figure 7. Electron density maps of Zn3 in the $Pt_xPd_{15-x}Zn_{54}$ (where $x \approx 6$ (left), 7 (middle), and 10 (right)) calculated from F(obs). The yellow colored lines represent the refined modulation behavior of the Zn3 atom.

refinements. Superstructure solutions are not only a worse fit of the data, but also they are erroneous because they force a nonperiodic to periodic description. Moreover, the commensurate space group is highly dependent on the approximation, which displays a multitude of possible structural description. In this case of $Fmmm(\alpha 00)0s0$, the following subperiodic groups are possible: (a) *Amam* and *Aeam* (for $q = 5/8$) and (b) *F*2/*m* and *Fm*2*m* (for $q = 8/13$). The data to parameter ratios improve dramatically as a result of treating the structures as incommensurate composites. So we consider $(Pd_xZn_{15-x})Zn_{54}$ (where $x \approx 6$, 7, 10) as effectively incommensurate, but the deviation from the translation periodicity of the reciprocal lattice may be outside the accuracy of the experiments. In the description of the structure of composite compounds, a commensurate approximation is used. The smallest but most reasonable commensurate approximation to the incommensurate structure is an 8-fold superstructure along the axis *a*. This is the result of an approximation of the measured $q \approx 0.627a^*$ to $q = (5/8)a^*$, and it produces an *a* axis of ~34.1 Å for $(Pt_xPd_{15-x})Zn_{54}$ (where $x \approx 6$) in the 3D structure description.

In this approximation, the composite structure can be described by a pentagonal antiprismatic column with a zigzag chain of Zn atoms extended inside the column (Figure 1). The chain of Zn atoms inside the columns is dancing along the *ab* plane but fixed by symmetry in the *c* direction. The structure is subdivided into two subsystems similarly to Nowotny's chimney-ladder phases.[30−32] The pentagonal antiprismatic frame forms the "chimney," and the zigzag chain of Zn3 atoms forms the "ladder" inside the chimney.

Occupancy modulations occur on two specific atomic sites—M1 and M′1. A clear change is observed for the ordering of the partial occupancy Pt and Pd on the M1 atomic site, which was modeled by three occupational modulations (c.f. Table 2, Figures 2 and 4). Moreover, occupancy modulation on the M′1 (an alteration between a mixed (Pt/Pd)1 and Zn1) atomic site remains quite fixed, whereas the ratio of Pt and Pd content changes insignificantly with the change of Pt content throughout the homogeneity range (Table 2, Figures 3 and 5). The remaining two atomic sites, Zn2 and Zn3 (Figures 6 and 7), are unaffected by the insertion of Pt over the homogeneity range.

In this section, we will deal with a comparison between $Pd_{24.3}Zn_{75.7}$ and $Pt_xPd_{15-x}Zn_{54}$ ($x \approx 6$, 7, 10) phases. All of them crystallized in the same superspace group. The complete structure is described by four atomic positions and their modulation in each structure. The modulation vector changes with the change of Pt content in the phase. It is noteworthy that in the binary $Pd_{24.3}Zn_{75.7}$ phase, the *q* vector is 0.6293(4). All of the structure is subdivided into two sublattices. Though different in composition, the ordered and disordered subsystems are the same as well.

In $Pd_{24.3}Zn_{75.7}$, the occupancy modulation occurs between Pd and Zn at M1 and M1′ sites. In the $Pt_xPd_{15-x}Zn_{54}$ ($x \approx 6$, 7, 10) phase, both the M1 and M1′ sites are also occupationally modulated. But in the ternary Pt−Pd−Zn system, M1 occurs between Pd1 and Pt1. M1′ alters between (Pt/Pd)1 and Zn1. Moreover, the ratio of Pt and Pd content varies noticeably parallel with the change of Pt content in the phase (Figure 2).

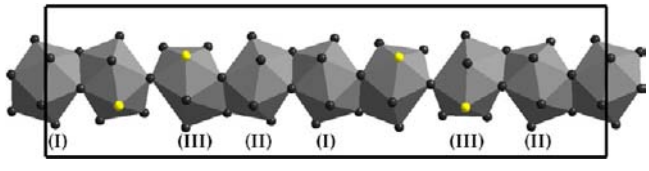

Figure 8. Representation of the chain of M1-centered clusters at height $c = 1/2$ connected by either faces or edges of icosohedra (I displays regular, II displays nearly regular, and III displays distorted icosohedra) in the $Pd_{24.3}Zn_{75.7}$ viewed along the *c* direction.

dx.doi.org/10.1021/ic301326p | *Inorg. Chem.* 2012, 51, 9893−9901

In the commensurate model, the disorder phenomenon, more precisely occupancy modulation of the solid solution, is correlated with the composition and confined to the pentagonal antiprismitic column of two different subsystems. The zigzag chain of Zn3 remains unaffected by Pt incorporation in the ternary Pt−Pd−Zn system.

M1 centered clusters in the $Pd_{24.3}Zn_{75.7}$ form either a chain of edges sharing or a faces sharing icosohedra (Figure 8). Note that in the $Pd_{24.3}Zn_{75.7}$, the Pd-rich central M1 atom has a Pd-poor but regular polyhedral environment. For an M1 centered Pd-poor site, the surrounding polyhedra are Pd-rich and distorted.[23]

In the Pt poor samples with composition $Pt_xPd_{15-x}Zn_{54}$ ($x \approx 6, 7$), Pt preferred to substitute Pd at the M1 site of the binary $Pd_{24.3}Zn_{75.7}$, which is encapsulated by regular icosohedra (I; c.f. Figure 9a and b; see also Figure 10). Furthermore, in the

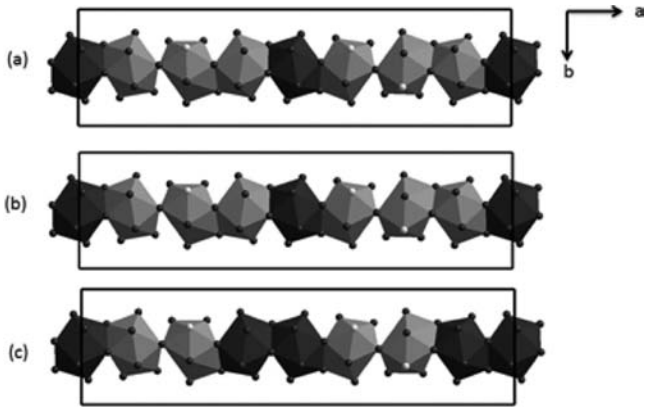

Figure 9. Representation of the chain of M1-centered clusters connected by either faces or edges of icosohedra in the (a) $Pt_xPd_{15-x}Zn_{54}$ (where $x \approx 6$), (b) $Pt_xPd_{15-x}Zn_{54}$ (where $x \approx 7$), and (c) $Pt_xPd_{15-x}Zn_{54}$ (where $x \approx 10$) at height $c = 1/2$ viewed along the c direction. Zn atoms are shown in dark gray, Pd in yellow, and mixing of (Pt/Pd) in light gray, respectively.

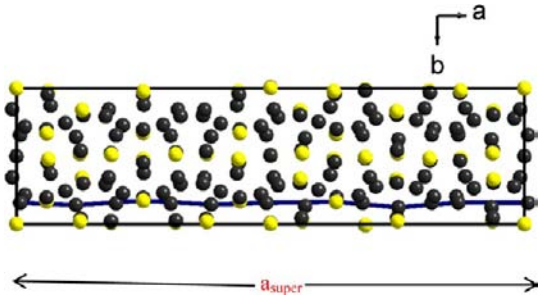

Figure 10. The structure of $Pd_{24.3}Zn_{75.7}$. An eight-atom chain of M1′ atoms along the c axis is discerned.

Pt-rich specimen of composition $Pt_xPd_{15-x}Zn_{54}$ ($x \approx 10$), Pt replaced the Pd site, which is covered by a nearly regular icosahedral site (II; c.f. Figure 9c) along with a Pd (M1) site which is surrounded by regular polyhedral (I). Interestingly, the more Pd is replaced by Pt in the phase, the more regular are the platimum centered icosahedra at M1 (0 0 0) (Figure 9). Closer inspection of the surroundings of the M1 site discerns that the Pt centered polyhedra are always surrounded by 12 zinc atom. Note that Pt is more electronegative than Pd and Zn (Zn, Pd, and Pt are 1.65, 2.20 and 2.28, respectively in the Pauling scale). An effect of charge balance may be the governing factor for such an occurrence.

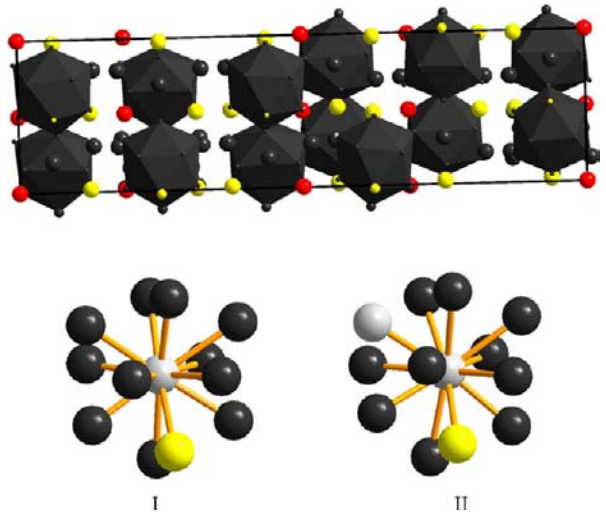

Figure 11. (Top) Representation of the (Pt/Pd)1-centered regular icosohedra in the $Pt_xPd_{15-x}Zn_{54}$ (where $x \approx 6$), viewed along the c direction. (Bottom) I and II display (Pt/Pd)-poor and -rich atomic environments at about M1′, respectively. Zn atoms are shown in dark gray, Pd in yellow, and mixing of (Pt/Pd) in light gray, respectively.

In the samples with composition $Pt_xPd_{15-x}Zn_{54}$ ($x \approx 6, 7, 10$), Pt attacks Pd only at the M1′ site. The M1′-centered clusters form more or less regular icosohedra (Figure 11) if the cluster is centered by a mixed (Pt/Pd)1 atom. The (Pt/Pd)-rich central M1′ atom has a Pd- and/or Pt-poor environment. For M1′, the (Pd/Pt)- poor site is coordinated by Pd and/or Pt-rich surroundings (Figure 11, I and II).

We assume that disorders on various sites are crucial to keep the vec nearly constant in terms of Hume−Rothery stabilization. Chemically speaking, an extended structure is a Hume−Rothery structure if (a) its electronic structure depends primarily on s- and p-orbital interactions and (b) the s- and p-electron count is near that of Cu_5Zn_8 (about 1.62 e/atom). This means that d orbitals of the constituent atomic sites are filled and for the most part not involved in bonding. An approach is simply to fill the d orbitals completely.

Hence, we take, for Pt and Pd, 0 e^- and, for Zn, 2 e^- into account. The occupancy modulation between Pt and Pd on various crystallographic positions retains the vec nearly constant throughout the entire homogeneity range. The fact is that the modulation between Pt and Pd at the M1 site does nothing. Note that sizes of Pd and Pt are similar (for Pd and Pt, metallic radii are 138 and 138.5 pm, respectively). There may be an electronic driving force for the observed ordering of partial occupancy of Pd and Pt due to the variation of the valence d orbital energies, but the modulation behavior of the (Pt/Pd)1 and Zn1 atoms is important and yields a homogeneous distribution throughout the phase.

SUMMARY

The structures of incommensurately modulated composite compounds $(Pt_xPd_{15-x})Zn_{54}$ (where $x \approx 6, 7, 10$) have been solved from X-ray single crystal diffraction data using a (3 + 1)D super space description. The structures are fully described by four independent atomic positions. The refinement model with changing the modulation vectors may allow us to refine any intergrowth structure $(Pt_xPd_{15-x})Zn_{54}$ in the Pd−Zn−Pt system if we are able to synthesize. The space group is unaffected by changes of the q vector. Hence, the phases described here

dx.doi.org/10.1021/ic301326p | Inorg. Chem. 2012, 51, 9893−9901

are isostructural in (3 + 1)D. The structure can be described in terms of pentagonal antiprismatic columns parallel to [100] running with a zigzag chain of zinc (Zn3) atoms using a commensurate approximation of the incommensurate structure.

EXPERIMENTAL SECTION

Single-phase samples $(Pt_xPd_{15-x})Zn_{\sim 54}$ with nominal composition x_{Pt} = 0, 0.08, 0.10, 0.14, and 0.22 were synthesized using conventional solid state techniques. The preparations were carried out on a 0.3 g scale from Pt (99.99%,ABCR), Pd (99.99%, ABCR), and Zn (99.9999%, Chempur) in previously outgassed, evacuated quartz glass ampules (3 cm long, 0.8 cm in diameter). The metals were heated at a rate of 194.4 K h^{-1} up to 1273 K and were kept at this temperature for 2 h. Hereafter, the temperature was reduced to 823 K at a rate of 90 K h^{-1} and annealed at this temperature over the course of 5 days, after which the ampules were either quenched in water or cooled to ambient temperature. Products obtained from these reactions were silvery, brittle, and stable in the air. Products were characterized by single crystal diffraction methods as well as energy dispersive X-ray spectroscopy (EDS).

In order to get reliable information about the γ-brass related zinc-rich phases and their homogeneity range, five distinct single crystals of $(Pt_xPd_{15-x})Zn_{\sim 54}$ were studied at room temperature by means of single crystal X-ray diffraction. The diffraction intensities were measured with a four circle diffractometer (X-calibur, Eos) equipped with graphite monochromatized Mo Kα radiation. The intensities could approximately be indexed on the basis of a *C*-centered orthorhombic super cell for all the samples.

ASSOCIATED CONTENT

Supporting Information

X-ray crystallographic files for C1, C2, and C3 in CIF file format are available free of charge via the Internet at http://pubs.acs.org. Crystallographic data for compounds C1, C2, and C3 have been deposited with the Cambridge Crystallographic Data Centre under CCDC 886159 (C1), 886158 (C2), and 886157 (C3).

AUTHOR INFORMATION

Corresponding Author

*Tel.: +46462224769. Fax: +46462224012. E-mail: Partha.Jana@polymat.lth.se.

Notes

The authors declare no competing financial interest.

ACKNOWLEDGMENTS

The authors wish to thank VR, the Swedish National Science Reasearch Council for the financial support.

REFERENCES

(1) Hume-Rothery, W. *J. Inst. Metals* **1926**, *35*, 309.
(2) Hume-Rothery, W.; Mabbott, G. W.; Channel-Evans, K. M. *Philos. Trans. R. Soc. London, Ser. A* **1934**, *233*, 1.
(3) Hume-Rothery, W.; Raynor, G. V. *The Structure of Metals and Alloys*; Institute of Metals: London, 1954.
(4) Bradley, A. J.; Thewlis, J. *Proc. R. Soc. London, Ser. A* **1926**, *112*, 678.
(5) Asahi, R.; Sato, H.; Takeuchi, T.; Mizutani, U. *Phys. Rev. B* **2005**, *71*, 165103.
(6) Westgren, A.; Phragmén, G. *Metallwirtsch., Metallwiss., Metalltech.* **1928**, *7*, 700−703.
(7) Westgren, A. F.; Phragmén, G. *Trans. Faraday Soc.* **1929**, *25*, 379−385.
(8) Asahi, R.; Sato, H.; Takeuchi, T.; Mizutani, U. *Phys. Rev. B* **2005**, *72*, 125102.
(9) Westman, S. *Acta Chem. Scand.* **1965**, *19*, 1411−1419.
(10) Johansson, A.; Ljung, H.; Westman, S. *Acta Chem. Scand.* **1968**, *22*, 2743.
(11) Edström, V.-A; Westman, S. *Acta Chem. Scand.* **1969**, *23*, 279−285.
(12) Harbrecht, B.; Thimmaiah, S.; Armbrüster, M.; Lee, S.; Pietzonka, C. *Z. Anorg. Allg. Chem.* **2002**, *628*, 2744−2749.
(13) Belin, C. H. E.; Belin, R. C. H. *J. Solid State Chem.* **2000**, *151*, 85−95.
(14) Brandon, J. K.; Brizard, R. Y.; Chieh, P. C.; McMillam, R. K.; Pearson, W. B. *Acta Crystallogr., Sect. A* **1974**, *30*, 1412−1417.
(15) Heidenstam, O.; Johansson, A.; Westman, S. *Acta Chem. Scand.* **1968**, *22*, 653−661.
(16) Gourdon, O.; Miller, G. *J. Chem. Mater.* **2006**, *18*, 1848−1856.
(17) Gross, N.; Kotzyba, G.; Künnen, B.; Jeitschko, W. *Z. Anorg. Allg. Chem.* **2001**, *627*, 155−163.
(18) Arnberg, L.; Westman, S. *Acta Chem. Scand.* **1972**, *26*, 513−517.
(19) Gourdon, O.; Izaola, Z.; Elcoro, L.; Petricek, V.; Miller, G. *J. Philos. Mag.* **2006**, *86*, 419−425.
(20) Morton, A. *Phys. Status Solidi A* **1974**, *23*, 275.
(21) Thimmaiah, S.; Conrad, M.; Lee, S.; Harbrecht, B. *Z. Anorg. Allg. Chem.* **2004**, *630*, 1762.
(22) Schmidt, J. T.; Lee, S.; Fredrickson, D. C.; Conrad, M.; Sun, J.; Harbrecht, B. *Chem.—Eur. J.* **2007**, *13*, 1394−1410.
(23) Gourdon, O.; Izaola, Z.; Elcoro, L.; Petricek, V.; Miller, G. J. *Inorg. Chem.* **2009**, *48*, 9715−9722.
(24) Morton, A. *Phys. Status Solidi A* **1977**, *44*, 205.
(25) Morton, A. *Phys. Status Solidi A* **1976**, *33*, 395.
(26) Morton, A. *Acta Metall.* **1979**, *27*, 863.
(27) Armbrüster, M.; Harbrecht, B.; Lee, S. *Book of Abstracts*; ECSSC: Oslo, Norway, 2001.
(28) Petricek, V.; Dusek, M.; Palatinus, L. *The Crystallographic Computing System, Jana2006*; Institute of Physics: Praha, Czech Republic, 2006.
(29) Palatinus, L.; Chapuis, G. *J. Appl. Crystallogr.* **2007**, *40*, 786−790.
(30) Wittmann, A.; Nowotny, H. *J. Less-Common Met.* **1965**, *9*, 303.
(31) Hayward, M. A.; Ramirez, A. P.; Cava., R. J. *J. Solid State Chem.* **2002**, *166*, 389−394.
(32) Jeitschko, W.; Parthé, E. *Acta Crystallogr.* **1967**, *22*, 417.